Validating Smartphone-Based 3D Head Models for Precision EEG Source Localization

Suranjita Ganguly
Dept. of Biomedical Engineering
Indian Institute of Technology Hyderabad
Hyderabad, India
bm19resch11002@iith.ac.in

Malaaika Mihir Chhaya
Dept. of Biomedical Engineering
Indian Institute of Technology Hyderabad
Hyderabad, India
malaaikachhaya@hotmail.com

Ankita Jain
Dept. of Biomedical Engineering
Indian Institute of Technology Hyderabad
Hyderabad, India
jaina865@gmail.com

Aditya Koppula
Dept. of Physiology
ESIC Medical College and Hospital Hyderabad
Hyderabad, India
aditya2171985@gmail.com

Mohan Raghavan
Dept. of Biomedical Engineering
Indian Institute of Technology Hyderabad
Hyderabad, India
mohanr@bme.iith.ac.in

Kousik Sarathy Sridharan
Dept. of Biomedical Engineering
Indian Institute of Technology Hyderabad
Hyderabad, India
ks@bme.iith.ac.in

***Abstract*— Accurate EEG source localisation requires subject-specific head geometry and precise electrode positions. Conventional digitization methods rely on specialised hardware such as electromagnetic trackers or 3D scanners, which increase experimental cost and complexity. This work presents a smartphone video–based photogrammetry framework for reconstructing subject-specific 3D head-surface models for EEG electrode registration. The method reconstructs head geometry from monocular video while incorporating blur detection and frame filtering to improve reconstruction robustness under realistic recording conditions. The resulting meshes are used to extract electrode positions and generate subject-specific EEG montages for source localisation. The approach was evaluated in a vibrotactile stimulation experiment involving ten participants. Photogrammetry-derived head models were validated against reference models obtained with a standard 3D scanner. Source localization results obtained from both models showed strong agreement, with root mean square errors of 0.035 mm and 0.037 mm for the left and right hemispheres, respectively. These findings demonstrate that smartphone video–based photogrammetry provides a practical and low-cost alternative for obtaining accurate head-surface models for EEG source modelling.**

Keywords—photogrammetry, EEG, source localization

I. Introduction

Source modelling is widely employed in EEG and MEG analysis to estimate the underlying cortical activity and their functional relevance [1], [2] By projecting scalp potentials back to their probable neural generators, this approach enables the investigation of brain dynamics at the source level and better interpretation of the findings.

Accurate source reconstruction requires a realistic representation of the subject's head geometry together with the precise spatial arrangement of EEG electrodes on the head surface. Consequently, two key pieces of subject-specific information are necessary [3] . The first is anatomical data describing the geometry of the head and cortex, typically obtained from structural magnetic resonance imaging (e.g., T1-weighted scans), which allows realistic modelling of the head volume for forward computations. The second is the precise three-dimensional position of EEG electrodes fitted on the subject, usually measured during the experiment.

Electrode positions are traditionally digitized using dedicated hardware systems, such as electromagnetic tracking devices [4], [5] or gold standard 3D scanners like EinScan Pro+ (Shining 3D) [6] that directly capture the surface geometry of the head. While these approaches can provide accurate measurements, they require expensive equipment and often increase experimental time, as electrode digitization must typically be performed while the subject is wearing the EEG cap. As an alternative, camera-based photogrammetry has emerged as a more accessible and cost-effective approach [7], [8]. In this method, the three-dimensional head surface and electrode locations are reconstructed from multiple two-dimensional images captured from different viewing angles using geometric reconstruction techniques. Unlike hardware-based digitization or scanning systems, camera-based photogrammetry does not require specialised equipment, making it a flexible and low-cost solution for obtaining electrode coordinates for source modelling.

However, existing photogrammetry systems often rely on multi-camera arrangements or carefully controlled single-camera and mirror-based setups [9]–[12] to ensure sufficient and contiguous spatial sampling of the head surface. Such configurations increase acquisition complexity and limit practical deployment.

An alternative and more flexible strategy is to acquire a continuous video of the subject's head and subsequently extract frames for reconstruction, enabling dense and uniform spatial sampling without specialised camera arrangements. Although such an attempt has been made once before, [13] the pipeline used 3D-printed head-surface which is be default stationery. In a real-life scenario, the subject would not be able to hold still throughout the duration of filming, and would introduce additional blurring, degrading 3D-reconstruction quality.

We present a video-based processing pipeline designed to automatically reconstruct subject-specific head surface models in 3D from smartphone video recordings. The proposed framework consists of three key stages. First, the head surface is reconstructed using an automated photogrammetry workflow that operates without manual intervention. Second, a blur-detection and frame filtering step identifies and removes low-quality frames that could negatively affect reconstruction accuracy under practical recording conditions. Third, the video sequence is resampled to ensure adequate spatial coverage of the head surface after blurred frames have been discarded. Furthermore, we evaluated the pipeline in a somatosensory stimulation experiment involving 10 participants, and analysed the cortical response to vibrotactile stimulation. For each participant, 3D head-surface models were reconstructed from

the recorded smartphone videos. High-precision scans acquired using the EinScan Pro+ (Shining3D) were used as reference ground-truth models for validation. The collected EEG data from the somatosensory paradigm was source-localised using the reconstructed geometries, and the performance of the pipeline was evaluated through statistical analyses described in the subsequent sections.

II. Experimental Set-up

A. Experimental set-up

Ten volunteers from the institute participated in the validation study. Ethical approvals were obtained from the institutional ethics committee.

The stimulation protocol consisted of two parts (Fig. 1): delivery of vibrotactile (VBT) stimulation and obtaining of head-surface geometry. Vibrotactile stimuli were delivered on the index finger. Each stimulus consisted of a 21 Hz vibration lasting 100 ms and was presented 200 times with an inter-stimulus interval of 900 ms.

Afterward, with the electrode cap still fitted on the subject's head, the head was first scanned using the 3D scanner, followed by recording a video using a smartphone for photogrammetry.

B. Data acquisition

The stimulation set-up was obtained from g.tec medical engineering GmbH. A 122-channel EEG cap, g.GAMMAcap, was fitted on each participant for EEG acquisition. In addition, two electrooculogram (EOG) channels (horizontal and vertical) and one electrocardiogram (ECG) channel were recorded to facilitate removal of ocular and cardiac artifacts from the EEG signals. Electrophysiological signals were amplified using the g.HIamp.

For stimulation, the g.VIBROstim stimulator was attached to the index finger of the participant.

Electrophysiological signals were sampled at 1200 Hz. Trigger signals were recorded separately at 32 Hz and later upsampled to 1200 Hz during post-processing to align with the EEG data.

To obtain the 3D head geometry, the following were collected for each participant: (a) a high-precision 3D scan used as the ground-truth model (hereafter referred to as G1), and (b) a smartphone video used to generate video-based photogrammetry models (hereafter known as M_{1080}). For the G1 acquisition, the standard scanner EinScan Pro+ (Shining3D) [14] was used to capture the head surface. Usage of the scanner involved calibration with the manufacturer-provided calibration board and was operated in handheld rapid-scan mode, which provides a nominal precision of approximately 0.3 mm according to the device manual.

For the photogrammetry-based reconstruction, Samsung Galaxy M32 smartphone camera was used for video recording at 1080p resolution and 30 fps. The investigator moved around the seated participant while maintaining focus on the head region, capturing a continuous 360° view of the EEG cap.

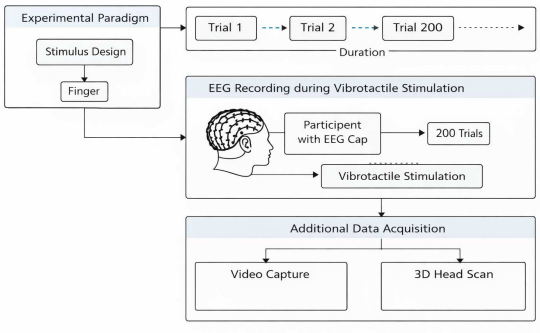

Fig. 1. A somatosensory experiment was conducted in which participants underwent 200 trials of vibrotactile stimulation. After recording the electrocortical signals, head geometry was captured using two approaches: a 1080p smartphone video and a 3D scan acquired with the Einscan Pro+ system. These data were then used to reconstruct head-surface meshes, enabling the identification and annotation of subject-specific electrode positions.

III. Method for Validating Framework

A. Video frame extraction

The input video was first decomposed into individual frames using the video capture and image input/output utilities provided by the OpenCV library. Frames were sequentially extracted and stored as JPEG images in a dedicated directory.

Since motion blur or defocus can significantly degrade the reliability of feature detection and matching during photogrammetric reconstruction, a frame quality filtering step was applied to remove blurred images. Each extracted frame was first converted to grayscale in order to simplify gradient computations and reduce computational complexity. Image sharpness was then quantified using the variance of the Laplacian operator, a commonly used focus measure in computer vision. The Laplacian operator measures the second-order spatial variation in image intensity, thereby emphasizing areas with abrupt changes that correspond to edges and fine structural features. In sharp images, these edges produce strong Laplacian responses, resulting in a high variance of the Laplacian values across the image. Conversely, blurred images tend to suppress high-frequency components and edges, producing smaller Laplacian responses and therefore lower variance values. For each frame, the variance of the Laplacian response was computed, and frames with values below a predefined threshold of 100 were classified as blurred and excluded from further processing.

Following this quality filtering step, the remaining frames were copied into a new working directory for subsequent photogrammetric reconstruction. Although the reconstruction pipeline supports temporal subsampling to reduce computational load, the sampling interval in the present study was set to 1, meaning that all frames that passed the blur detection step were retained. The original frame directory was deleted after filtering in order to reduce storage requirements. The final number of retained frames was recorded and used to parameterize later stages of the reconstruction pipeline.

B. Photogrammetric 3D Reconstruction

Three-dimensional reconstruction was performed using modules from the AliceVision framework [15]. Camera intrinsics and image metadata were initialized using the *cameraInit* module, which utilized the AliceVision camera sensor database together with the image directory. The resulting camera initialization file served as the input for all subsequent stages.

Local visual features were extracted using the *featureExtraction* module. Images were processed in batches

of 40 to control memory usage. Potentially overlapping image pairs were identified using the *imageMatching* module. The resulting candidate pair list was then used for feature correspondence estimation.

Feature correspondences were computed using the *featureMatching* module with approximate nearest-neighbour matching under an L2 metric. Geometric verification was performed using an RANSAC estimator with a fundamental matrix model and a distance ratio threshold of 0.8. When necessary, matching was executed in batches of 20 images.

Sparse structure-from-motion reconstruction was carried out using the *incrementalSfm* module, which simultaneously estimated camera poses and generated a sparse three-dimensional point cloud. The reconstruction output included camera pose parameters and the sparse point cloud in Alembic format.

For dense reconstruction, the sparse model was converted into a dense workspace using *prepareDenseScene*. Per-view depth maps were computed using *depthMapEstimation*, followed by refinement using *depthMapFiltering* to remove inconsistent estimates and improve geometric consistency. Finally, a dense point cloud and triangular surface mesh were generated using the meshing module. The mesh was further refined using *meshFiltering*, retaining only the largest connected component.

C. Electrode Annotation and Montage Generation

The reconstructed mesh was loaded into a custom graphical user interface implemented using the PyVista visualization library [16]. PyVista enabled interactive visualization of the three-dimensional head-surface mesh and allowed manual annotation of electrode positions directly on the mesh surface. The spatial coordinates of each annotated electrode were extracted from the mesh geometry and assigned corresponding electrode labels to generate a subject-specific EEG montage.

The recorded videos were processed using the method described in the previous section to generate a 3D head-surface model, referred to as M_{1080}. A structured-light 3D scan of the same subject, denoted G1, served as the reference model. Electrode positions were manually annotated on both meshes using the PyVista-based interface to obtain the corresponding three-dimensional electrode coordinates.

This resulted in two electrode configurations for the same VBT-based EEG recordings: one derived from the scanner-based model (G1) and the other from the photogrammetry-based model (M_{1080}). The EEG data were processed using two parallel pipelines, each employing the same preprocessing and source-analysis procedures but applied to their respective electrode configurations.

IV. Method for Validating Framework

A. EEG Processing

he EEG recordings were first filtered using a band-pass range of 1–300 Hz with a third-order Butterworth IIR filter. Power-line noise was removed with a notch filter at 50 Hz and its harmonics. Channels and time segments containing motion-related artifacts were identified and excluded from subsequent processing. Independent component analysis (ICA) was then performed to identify components corresponding to ocular (EOG) and cardiac (ECG) artifacts, which were removed before reconstructing the cleaned EEG signals. The resulting data were visually inspected to verify signal quality, and any remaining corrupted portions were discarded. Finally, the trigger stream was upsampled to match the EEG sampling rate of 1200 Hz, ensuring precise temporal alignment between stimulus events and the recorded electrophysiological signals.

The preprocessed EEG data were segmented into epochs using the stimulus trigger markers. Baseline correction was performed using a pre-stimulus interval from −200 ms to −50 ms, after which epochs were averaged to obtain subject-specific evoked responses.

The 3D model generated through G1 and M_{1080} were separately used for source reconstruction. The source reconstruction procedure followed the approach described in [17]. After estimating the cortical sources, the resulting activity was represented as source time courses (STCs), which correspond to time-varying activation at each cortical location. Each STC therefore reflects the temporal evolution of neural activity within a specific anatomical region. The cortical area defined as the region of interest (ROI) was

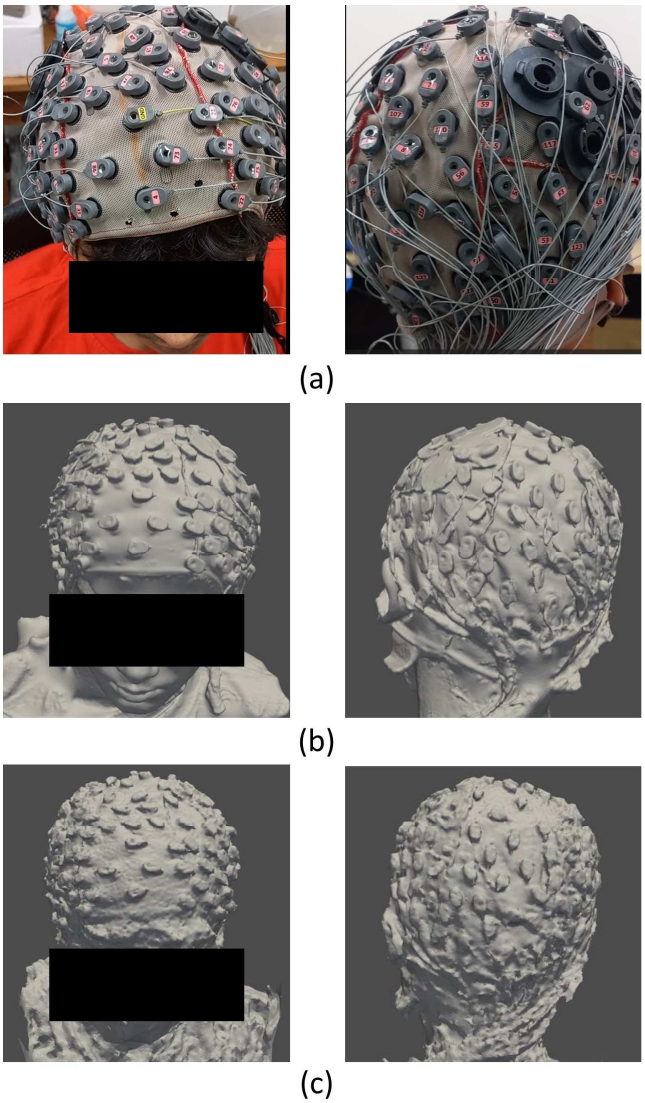

Fig. 2 Representative front and side views of a subject are presented for (a) a frame extracted from the input video, (b) the 3D model acquired using a 3D scanner, (c) the head model reconstructed via photogrammetry from the 1080p video, and (d) the model reconstructed using the proposed video-processing pipeline. The face of the participant has been obstructed for privacy purposes.

identified, and the associated source time course (STC) was extracted for each subject. These STCs were subsequently used in the validation analyses.

V. RESULTS

A. *Photogrammetry model vs 3D-scanned model: Structural analysis*

Fig. 2 presents representative front and side views illustrating the outputs obtained from the two reconstruction approaches. Fig. 2(a), shows the subject wearing the EEG electrode cap. The reference 3D head model obtained using the 3D scanner is shown in Fig. 2(b). Fig. 2(c) shows the reconstructed model using the photogrammetry method. The reconstructed surface preserves the overall head shape while also representing protrusions associated with the electrode housings. This model serves as a high-resolution reference representation of the subject-specific head surface and electrode layout. Figure 3(c) shows the head-surface model reconstructed using the proposed video-based photogrammetry pipeline from the 1080p smartphone recording. The reconstructed mesh successfully recovers the overall head geometry and the surface topology induced by the electrode cap. The electrode locations and cap structure are clearly visible in the reconstructed mesh, indicating that the pipeline is capable of preserving the spatial features required for electrode localisation.

A qualitative comparison between the two reconstructions demonstrates that the photogrammetry-based model closely resembles the scanner-derived model in terms of overall head shape and electrode distribution. While the scanner-based reconstruction provides slightly smoother surface detail, the photogrammetric reconstruction preserves sufficient geometric fidelity to identify electrode positions and head contours. These results demonstrate that the proposed monocular video-based reconstruction pipeline can generate subject-specific head-surface meshes suitable for subsequent electrode localisation and source modelling.

TABLE I
MEAN DISTANCES OF COM OF CORTICAL ACTIVITY FROM THE ORIGIN FOR THE 3D SCANNER (G1) AND PHOTOGRAMMETRY (M_{1080}) RECONSTRUCTED MODELS

	Mean distance of SI activity in mm (Left hemisphere)	**Mean distance of SI activity in mm (Right hemisphere)**
G1	0.112 ± 0 0.011	0.122 ± 0.011
M_{1080}	0.091 ± 0.018	0.092 ± 0.016
RMSE error	0.035	0.037

B. *Photogrammetry model vs 3D-scanned model: Source localisation*

The 3D models were utilized to estimate source time courses (STCs), which were visualized on an inflated cortical surface (Fig. 3). Consistent with prior findings on cortical responses to vibrotactile stimulation, activity was localized to the primary somatosensory (SI) cortex [18]–[21] for both G1 and M1080 (Fig. 3(a) and (b)).

The Euclidean distances of the center of mass (CoM) of SI cortical activity of G1 and M_{1080} are shown in Table I. The RMSE between the source activity estimates obtained using G1 and M1080 was 0.035 mm for the left hemisphere and

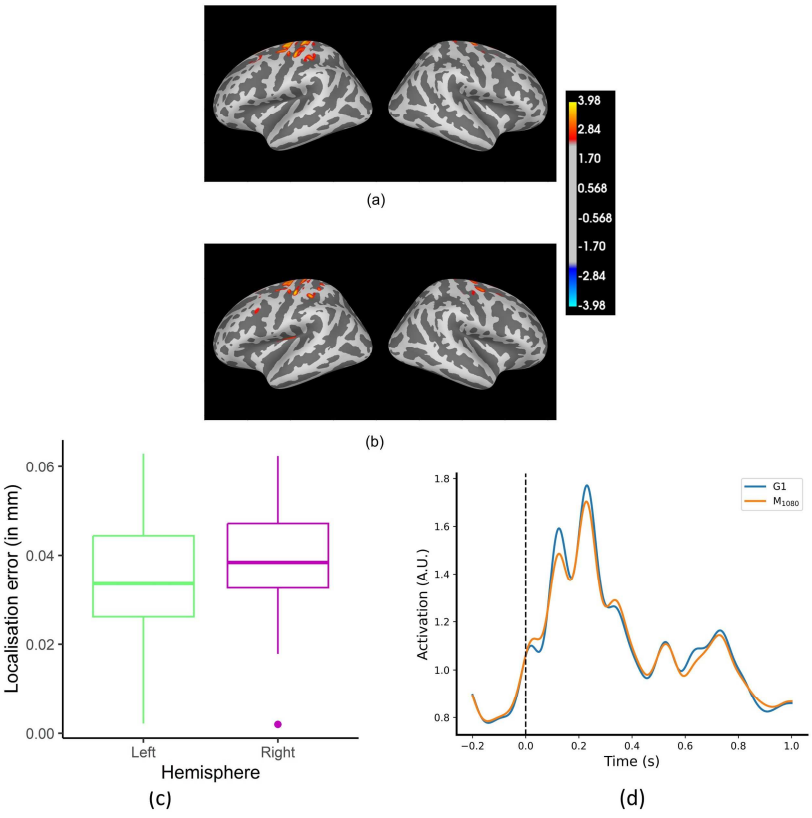

Fig. 3 The reconstructed source time course is shown for (a) G1 and (b) M_{1080}. (c) Localisation errors per hemisphere for M_{1080} is shown compared to G1 (d) The corresponding source time courses for both the models are shown. Minimal difference is observed between the models.

0.037 mm for the right hemisphere. The distances are visualised in Fig. 3(c). The corresponding source activity pertaining to the two models are visualized in Fig. 3(d).

VI. DISCUSSION

To assess the effectiveness of the proposed photogrammetry-based 3D reconstruction for source modelling, the generated meshes were compared against reference models acquired using a conventional 3D scanner [8], [16]. For validation, sensor positions were manually marked on both the photogrammetry-based and scanner-based meshes, and the Euclidean distances between corresponding electrode locations were then calculated. The results indicate high spatial agreement between the two reconstructions. The RMSE of the center of mass (CoM) of the estimated source activity was 0.035 mm in the left hemisphere and 0.037 mm in the right hemisphere.

This was followed by enforcing an experimental protocol designed to elicit neural activity in the somatosensory cortex wherein source activity obtained from both the photogrammetry-based model and the 3D-scanner based model were compared. Source reconstruction showed comparable results.

REFERENCES

[1] A. Højlund, M. V. M. V. M. V Petersen, K. S. K. S. K. S. Sridharan, and K. Østergaard, "Worsening of Verbal Fluency After Deep Brain Stimulation in Parkinson's Disease: A Focused Review.," *Comput. Struct. Biotechnol. J.*, vol. 15, pp. 68–74, 2017.

[2] K. S. Sridharan *et al.*, "Differentiated effects of deep brain stimulation and medication on somatosensory processing in Parkinson's disease," *Clin. Neurophysiol.*, vol. 128, no. 7, pp. 1327–1336, Jul. 2017.

[3] L. Koessler, T. Cecchin, O. Caspary, A. Benhadid, H. Vespignani, and L. Maillard, "EEG-MRI co-registration and sensor labeling using a 3D laser scanner," *Ann. Biomed. Eng.*, vol. 39, no. 3, pp. 983–995, 2011.

[4] C. Whalen, E. L. Maclin, M. Fabiani, and G. Gratton, "Validation of a method for coregistering scalp recording locations with 3D structural MR images," *Hum. Brain Mapp.*, vol. 29, no. 11, pp. 1288–1301, 2008.

[5] B. H. Brinkmann, T. J. O'Brien, M. A. Dresner, T. D. Lagerlund, F. W. Sharbrough, and R. A. Robb, "Scalp-recorded EEG localization in MRI volume data," *Brain Topogr.*, vol. 10, no. 4, pp. 245–253, 1998.

[6] L. Koessler, T. Cecchin, E. Ternisien, and L. Maillard, "3D handheld laser scanner based approach for automatic identification and localization of EEG sensors," *2010 Annu. Int. Conf. IEEE Eng. Med. Biol. Soc. EMBC'10*, pp. 3707–3710, 2010.

[7] S. Y. Shirazi and H. J. Huang, "More Reliable EEG Electrode Digitizing Methods Can Reduce Source Estimation Uncertainty, but Current Methods Already Accurately Identify Brodmann Areas," *Front. Neurosci.*, vol. 13, no. November, pp. 1–14, 2019.

[8] G. A. Taberna, M. Marino, M. Ganzetti, and D. Mantini, "Spatial localization of EEG electrodes using 3D scanning," *2D Mater.*, pp. 0–23, 2018.

[9] O. Györfi *et al.*, "Accuracy of high-density EEG electrode position measurement using an optical scanner compared with the photogrammetry method," *Clin. Neurophysiol. Pract.*, vol. 7, pp. 135–138, 2022.

[10] T. Clausner, S. S. Dalal, and M. Crespo-García, "Photogrammetry-based head digitization for rapid and accurate localization of EEG electrodes and MEG fiducial markers using a single digital SLR camera," *Front. Neurosci.*, vol. 11, no. MAY, pp. 1–12, 2017.

[11] U. Baysal and G. Şengül, "Single Camera photogrammetry system for EEG electrode identification and localization," *Ann. Biomed. Eng.*, vol. 38, no. 4, pp. 1539–1547, 2010.

[12] S. Qian and Y. Sheng, "A single camera photogrammetry system for multi-angle fast localization of EEG electrodes," *Ann. Biomed. Eng.*, vol. 39, no. 11, pp. 2844–2856, 2011.

[13] I. Mazzonetto, M. Castellaro, R. J. Cooper, and S. Brigadoi, "Smartphone-based photogrammetry provides improved localization and registration of scalp-mounted neuroimaging sensors," *Sci. Rep.*, vol. 12, no. 1, pp. 1–14, 2022.

[14] S. Ganguly, M. M. Chhaya, A. Jain, A. Koppula, M. Raghavan, and K. S. Sridharan, "Mark3D - A semi-automated open-source toolbox for 3D head- surface reconstruction and electrode position registration using a smartphone camera video.," *Med. Biol. Eng. Comput.*, Nov. 2024.

[15] AliceVision, "Meshroom: A 3D reconstruction software." 2018.

[16] C. Sullivan and A. Kaszynski, "PyVista: 3D plotting and mesh analysis through a streamlined interface for the Visualization Toolkit (VTK)," *J. Open Source Softw.*, vol. 4, no. 37, p. 1450, 2019.

[17] S. Ganguly, A. Koppula, and K. S. Sridharan, "Mid-Latency Cortical Encoding of Arousal in Vibrotactile Stimulation: Evidence from Somatosensory cortex Source Activity," *Next Res.*, p. 101639, 2026.

[18] M. Y. Kim, H. Kwon, T. H. Yang, and K. Kim, "Vibration Alert to the Brain: Evoked and Induced MEG Responses to High-Frequency Vibrotactile Stimuli on the Index Finger of Dominant and Non-dominant Hand," *Front. Hum. Neurosci.*, vol. 14, no. November, 2020.

[19] H. Burton, R. J. Sinclair, and D. G. McLaren, "Cortical activity to vibrotactile stimulation: An fMRI study in blind and sighted individuals," *Hum. Brain Mapp.*, vol. 23, no. 4, pp. 210–228, 2004.

[20] R. C. Coghill *et al.*, "Distributed processing of pain and vibration by the human brain," *J. Neurosci.*, vol. 14, no. 7, pp. 4095–4108, 1994.

[21] R. Hari, "Evoked potentials elicited by long vibrotactile stimuli in the human EEG," *Pflügers Arch. Eur. J. Physiol.*, vol. 384, no. 2, pp. 167–170, 1980.